Dynamic Impedance Measurements During Radio-Frequency Heating of Cornea

Bernard Choi*, Jihoon Kim, Ashley J. Welch, and John A. Pearce, *Senior Member, IEEE*

***Abstract*—Hyperopia affects approximately 25% of the population. The aim of different heating modalities for the treatment of hyperopia is to steepen the central curvature of the cornea. Conductive keratoplasty (CK) involves the placement of radio-frequency (RF) lesions around a 7-mm-diameter ring concentric with the pupil of the eye. Dynamics of lesion formation during CK depend on corneal electrical impedance, which is expected to change during each 600-ms-long macropulse.**

The purpose of this study was to measure impedance dynamics during CK. RF lesions were made in *in vitro* porcine eyes at different power settings. Voltage and current measurements were acquired using a high-speed computer-based data acquisition system. Root-mean-square voltages (V_{RMS}) and currents (I_{RMS}) were calculated for each micropulse, and impedance was determined by calculating the quotient $V_{\mathrm{RMS}}/I_{\mathrm{RMS}}$. Initial corneal impedance *in vitro* was approximately 2000 Ω. During the macropulse, impedance decreased initially due to increased mobility of conductive ions. At higher power settings (e.g., $>$70%, or maximum peak-to-peak voltage of 233 V), impedance increased after the initial decrease, indicative of local water vaporization and/or tissue coagulation. Preliminary impedance data obtained for *in vivo* porcine eyes were similar in magnitude to the *in vitro* values.

***Index Terms*—Cornea, impedance measurements, radio-frequency, thermal damage.**

I. Introduction

HYPEROPIA is caused by insufficient curvature of the cornea so that the focal point of image formation by the ocular optical structures is posterior to the retina. Approximately 22%–27% of the population are hyperopic [1]. Two approaches to this problem are currently being investigated. The first, laser thermokeratoplasty (LTK), uses a Holmium–YAG (Ho : YAG) laser at a wavelength of 2.1 μm to create lesions on concentric rings in the periphery of the cornea [2], [3] (Fig. 1) The second, conductive keratoplasty (CK) [Refractec, Inc., Irvine, CA] employs monopolar radio-frequency (RF) current to create lesions at similar locations.

Manuscript received October 25, 2001; revised May 28, 2002. This work was supported in part by grants from the Air Force Office of Scientific Research through MURI from DDR&E (F49620-98-1-0480), the Texas Higher Education Coordinating Board (BER-ATP-253), the Albert and Clemmie Caster Foundation, and Refractec, Inc. *Asterisk indicates corresponding author.*

*B. Choi was with the Department of Biomedical Engineering, The University of Texas at Austin, Austin, TX 78712 USA. He is now with Beckman Laser Institute, 1002 Health Sciences Road East, Irvine, CA 92612 USA (e-mail: bchoi@laser.bli.uci.edu).

J. Kim and A. J. Welch are with the Department of Biomedical Engineering, The University of Texas at Austin, Austin, TX 78712 USA.

J. A. Pearce is with the Department of Electrical and Computer Engineering, The University of Texas at Austin, Austin, TX 78712 USA.

Digital Object Identifier 10.1109/TBME.2002.805471

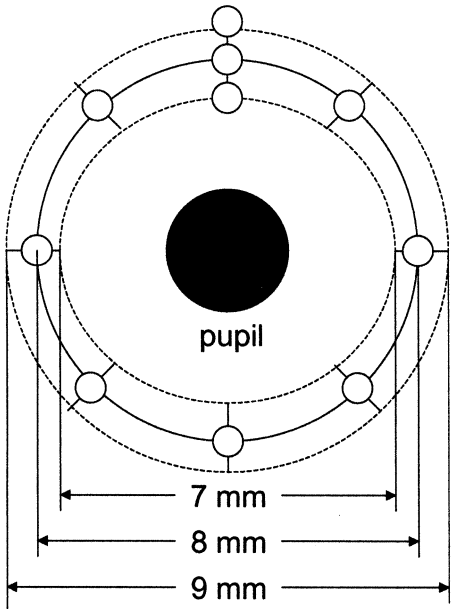

Fig. 1. Schematic of lesion placement for LTK and CK treatments. Typically, eight lesions are placed along an 8-mm-diameter ring that is concentric with the pupil of the eye. Lesions can also be placed along an inner (7-mm diameter) and outer ring (9-mm diameter). An example of multiple lesion placement is shown at the top of the figure (e.g., at the "12 o'clock position").

Regression of the initial eyesight correction is a problem in LTK procedures, particularly for younger patients and for patients requiring significant hyperopic correction [1]. CK apparently creates a more uniform and deeper heating which results in longer lasting shrinkage of stromal collagen. Pilot clinical studies have shown that CK treatments achieve accurate, stable results for correction of low levels of hyperopia [4].

In both methods thermally induced contraction of stromal collagen leads to a "purse-string" effect in the corneal periphery, increasing the curvature in the central region of the cornea [5]. Ideally, the end result of heating is full-thickness stromal heating for a sufficient time to induce collagen contraction to increase central corneal curvature. The thickness of the human stroma is $\sim$600–700 μm, and the stroma is composed of 75% water by mass [6]. The absorption of laser energy in LTK procedures is dominated by tissue water at the Ho : YAG wavelength. The $1/e$ penetration depth of Ho : YAG laser light in water is approximately 360 μm [7]. The tissue water content also has a strong affect on its electrical conductivity. Water vaporization is a governing physical process in both procedures.

The metal monopolar active electrode used in CK procedures is 90 μm in diameter and extends 450 μm out from a dielectric shoulder used to control electrode penetration (Fig. 2). The

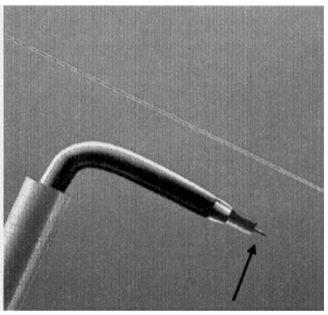

Fig. 2. Photograph of the Refractec probe. The tip (indicated by the black arrow) is 90 μm in diameter and 450 μm long. Courtesy of Refractec.

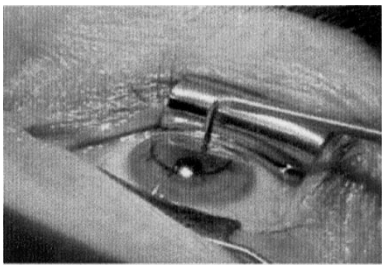

Fig. 3. Photograph of CK procedure. A speculum is used to hold the eyelids back. The corneal surface is marked with a purple pattern to indicate at what points RF lesions should be formed. Courtesy of Refractec.

probe is inserted into the corneal periphery at desired points (Fig. 3) and an eyelid speculum comprises the return (i.e., dispersive) electrode for the system. A 600-ms-long macropulse of RF energy is applied to each site (duration fixed by the RF generator). Each macropulse consists of exponentially damped sinusoidal RF pulses—fundamental frequency of 350 kHz—delivered at a nominal 8-kHz pulse repetition rate. After completion of a macropulse, the electrode is moved and inserted at the next site.

The rate of heat delivery to the cornea during a RF macropulse has not been sufficiently characterized. Measurements of average power delivered to *in vitro* bovine eyes with the CK unit indicate that the average power can change by a factor of 40 during a 600-ms macropulse [R. Stern, Stellartech Research Corporation (Sunnyvale, CA), unpublished data]. This decrease in power is attributed to a dynamic change in tissue impedance. If constant tissue properties are assumed, the actual RF dose can differ considerably from the expected dose. Measurements of electrical impedance can provide information on dynamic changes in power delivered to tissue. The purpose of this study is to measure voltage and current values during RF heating of *in vitro* and *in vivo* porcine corneas.

II. Materials and Methods

A. CK Unit

The RF generator (RCS-200, Refractec, Inc., Irvine, CA) emits macropulses of up to 1-s in duration. Each macropulse consists of micropulses, which are essentially damped 350-kHz sinusoidal waveforms (see Fig. 4). The amplitude of a set of micropulses is varied by changing the "Power" setting on the CK unit. "Power" is expressed as a percentage and represents the fraction of the maximum peak-to-peak voltage (333 V_{p-p}) delivered with each macropulse. Nominal clinical settings are 60% power (e.g., 200 V_{p-p}) and 600-ms macropulse duration.

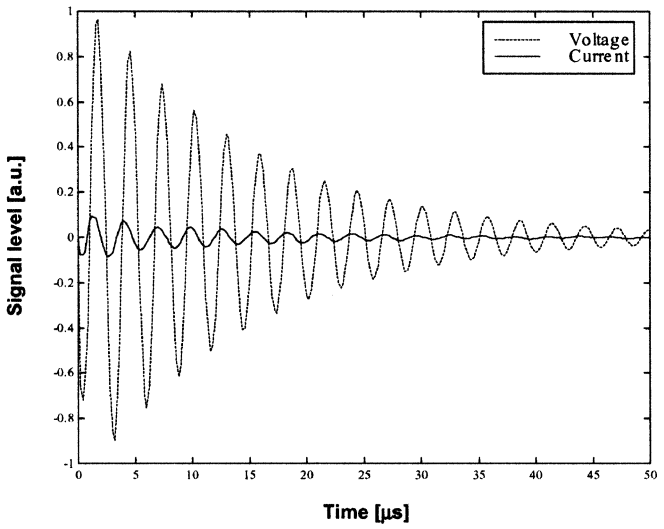

Fig. 4. Voltage and current waveforms taken during a single micropulse. Each micropulse is essentially a damped sinusoid oscillating at 350 kHz.

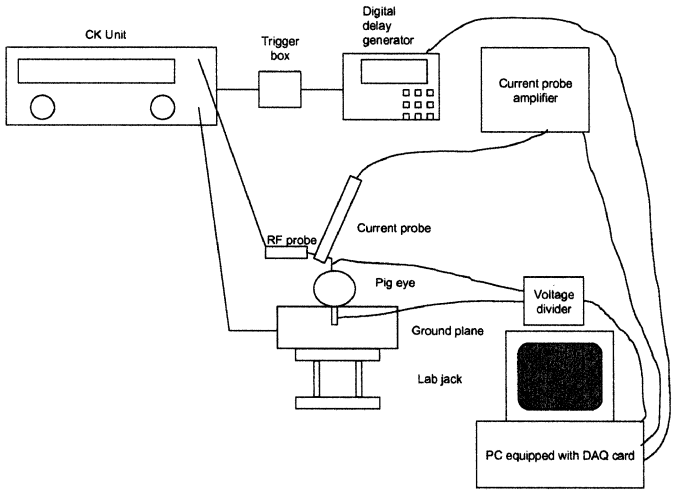

Fig. 5. Diagram of high-speed data acquisition system used to measure impedance during *in vitro* experiments. For *in vivo* measurements, the ground plane was replaced with an eyelid speculum.

B. Impedance Measurements

A PC-based data acquisition system (Fig. 5) was developed to acquire voltage and current waveforms during RF energy application to *in vitro* porcine eyes. A pulse generator (DG535, Stanford Research Systems, Sunnyvale, CA) was used to trigger simultaneously the CK unit and the data acquisition system. Voltage was measured across the eye using a custom 1 : 100 voltage divider. Current values were measured with a current probe (A6302, Tektronix, Beaverton, OR) and current probe amplifier (AM 503B, Tektronix, Beaverton, OR). Voltage and current data were acquired at 5 MHz/channel with a 12-bit data acquisition board (PCI-6110E, National Instruments, Austin, TX) and LabVIEW software (Version 6i, National Instruments, Austin, TX).

After preliminary measurements of voltage and current were measured from two *in vitro* pig eyes and custom-made resistive

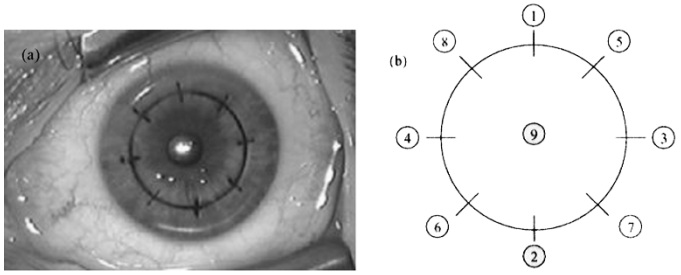

Fig. 6. (a) Photo and (b) diagram of pattern placed on corneal surface to indicate at what points RF lesions should be placed. The numbers in (b) (except for #9) indicate the order in which lesions are placed clinically and were applied in this study. The image in (a) is courtesy of Refractec.

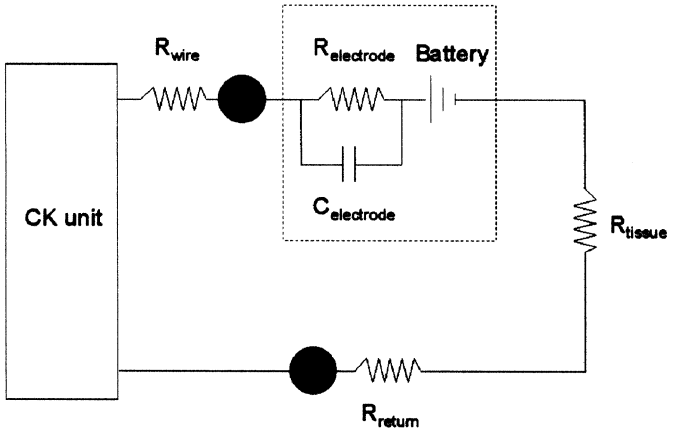

Fig. 7. Equivalent circuit diagram of RF setup. The solid black dots represent the location of measurement electrode placement. The dashed box encloses the equivalent circuit comprising the RF probe.

loads, final data was acquired during two sets of experiments on 23 eyes. The initial experiment involved measurements at the nominal 60% power, 600-ms macropulse duration settings. A subsequent experiment examined the effect of the power setting on impedance; measurements were taken over the range 30%–98% power (e.g., maximum $V_{p-p} = 100$–333 V).

1) In Vitro Experimental Geometry: In vitro porcine eyes were obtained from a local distributor and used within 24 hours of enucleation. The specimens were stored in 0.01 M phosphate-buffered saline at 4 °C until they were used. Each eyeball was placed in a heated water bath at 32 °C–37 °C for approximately five minutes. The eye was removed and placed in a metal suction ring which formed the ground plane. Suction was applied gently using a large syringe to fix the eyeball in place. Balanced salt solution (BSS) was injected into the aqueous humor to increase the intraocular pressure (IOP) so that the corneal surface was rigid. The IOP was not quantified.

A stainless-steel corneal marker was used to mark the corneal surface with gentian violet dye to guide positioning of the CK probe [Fig. 6(a)]. The corneal surface was wetted with four drops of BSS and dried with a Weck sponge; this was done to wash away excess dye.

The CK probe was inserted into the desired spot with sufficient pressure to depress the punctured region (as evident by formation of stress lines). The operator slowly withdrew the probe so that the 450-μm-long active region remained in the cornea but the stress lines were no longer visible. The order of lesion placement is shown in Fig. 6(b). In clinical operation, the central lesion [#9 in Fig. 6(b)] is not applied.

2) In Vivo Experimental Geometry: Voltage and current waveforms were acquired during procedures on two female minipigs according to an approved protocol by The University of Texas at Austin Animal Care and Use Committee. Each animal was tranquilized with a Telazol/xylazine mixture (100-mg Telazol/100-mL xylazine). The eyelids were held open with a speculum, which also served as the return path electrode for the CK unit. A drop of proparacaine hydrochloride (Alcaine, Alcon Laboratories Inc., Fort Worth, TX) was placed in the eye to keep the underlying nictatating membrane from closing during lesion placement. The gentian violet ring was marked on the cornea with the corneal marker and excess dye removed with a Weck sponge. Lesions were placed in the eye in a similar fashion to the *in vitro* experiments. Voltage and current signals were acquired during application of each lesion on the four eyes.

3) Signal Processing: All processing was done using LabVIEW 6i. The data were low-pass filtered with a second-order Butterworth filter ($f_c = 500$ kHz) to remove unwanted high frequency components and visually scanned to determine the starting point of each micropulse. Root-mean-square (RMS) voltages and currents were calculated for each micropulse and the impedance magnitude calculated as a function of micropulse number by dividing RMS voltage values by RMS current values.

In the *in vitro* time-resolved impedance curves, a low amplitude (e.g., approximately 5% of the calculated impedance) 60-Hz component was present. This may have been due to pickup of electrical noise by the metal suction ring that served as the return electrode. A 60-Hz filter was applied to the *in vitro* impedance data to remove the noise.

C. Electrode Interface Impedance

An important consideration in overall impedance measurement is the series impedance of the active electrode–tissue interface. Usually, at high frequencies (above about 20 kHz) the capacitive impedance of the electrode double layer is so small that the electrode interface appears as a small series resistance. However, because of the extremely small size and sharp tip of the RF active electrode one may question whether or not the fundamental frequency (350 kHz) is high enough to make that assumption in this case.

Since our measurements of impedance included the electrode interface impedance (Fig. 7), it was necessary to determine the significance of this impedance. A separate experiment (Fig. 8) was conducted to measure the effect of the interface as a function of frequency. Electrode interface impedance was measured over the frequency range of interest in a coaxial saline chamber with a Hewlett-Packard 4194A Impedance/Gain-Phase Analyzer (Agilent Technologies, Palo Alto, CA, overall accuracy 0.15%). The cylindrical outer chamber (19-mm diameter by 54-mm tall) was filled with 0.137 M saline solution (approximately 0.8%) which had a measured and calculated electrical conductivity of 1.39 S/m. The electrode interface impedance

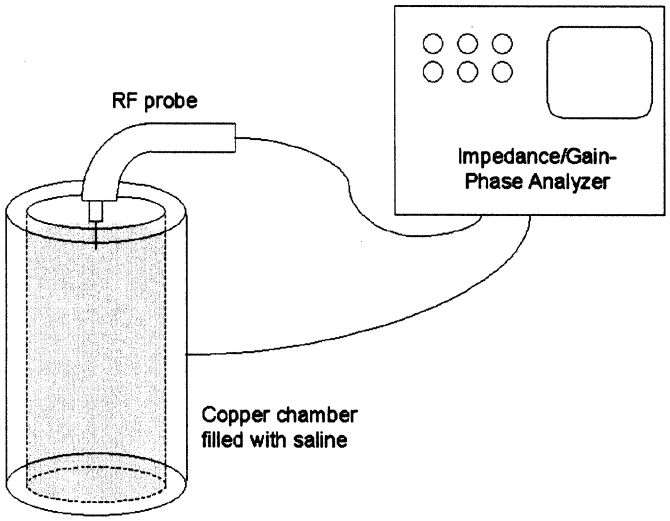

Fig. 8. Setup used to measure electrode interface impedance. Magnitude and phase spectra were measured using the CK probe as the signal electrode and a copper cylinder as the return electrode. The inner surface of the copper chamber was silvered. The frequency range covered was 100 kHz to 10 MHz.

spectrum was measured from 100 Hz to 10 MHz (logarithmic sweep) in the coaxial chamber.

III. Results

A. Electrode Interface Impedance

The measured impedance spectrum is shown in Fig. 9. The strong series capacitive component is seen for frequencies less than about 10 kHz. At 350 kHz the magnitude is 589 Ω and the phase angle is -5.3°. Since the impedance magnitude and phase angle at 350 kHz are in the frequency-independent regions of the respective spectra (Fig. 9), is acceptable to assume an essentially resistive contact at the fundamental frequency.

B. In Vitro Measurements

In the first set of *in vitro* experiments, 90 impedance curves were generated from voltage/current measurements. The initial mean impedance value was 1775 Ω (Fig. 10). During the 600-ms macropulse, the average impedance decreased from 1775 to $\sim$1350 Ω in approximately 150 ms. The impedance gradually increased over the next 450 ms to 1450 Ω.

A total of 45 impedance calculations were obtained at different power settings. The initial impedance was 2158 ± 157 Ω (Fig. 11). For a power setting of 30%, mean impedance stayed approximately constant [Fig. 11(a)]. As power increased from 30% to 70%, impedance values decreased to lower values during the entire macropulse. The impedance curves for 50% and 60% powers were similar in overall shape. For power settings of 80% to 98%, the impedance-time history was significantly different [Fig. 11(b)]. In general, the impedance decreased over the first 200 ms, after which it increased. At 80% power, the impedance at the end of the macropulse was equivalent to the initial value.

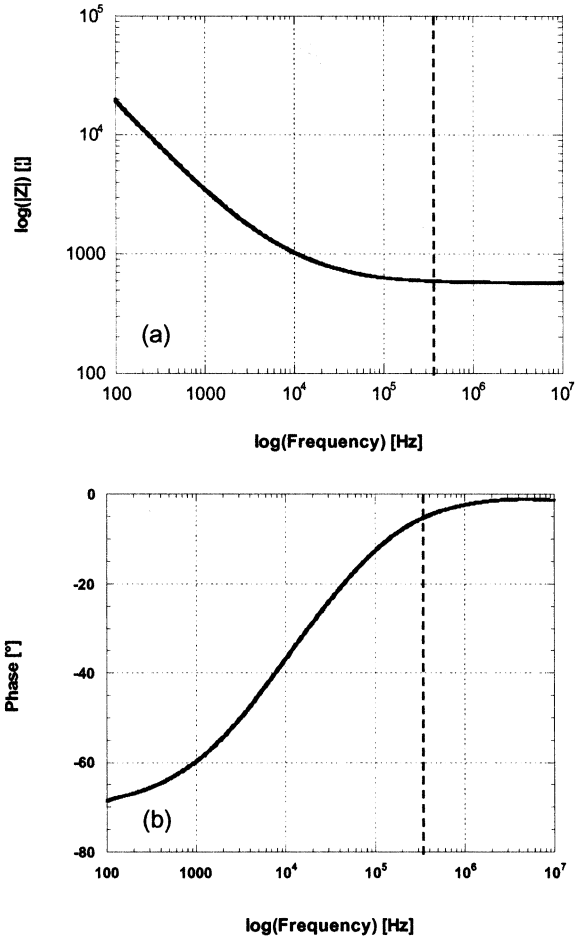

(b)

Fig. 9. Impedance spectrum of CK active electrode in saline. (a) Log–log plot of magnitude spectrum. (b) Semilog plot of phase angle spectrum. The dashed line represents the 350-kHz fundamental frequency used in this study.

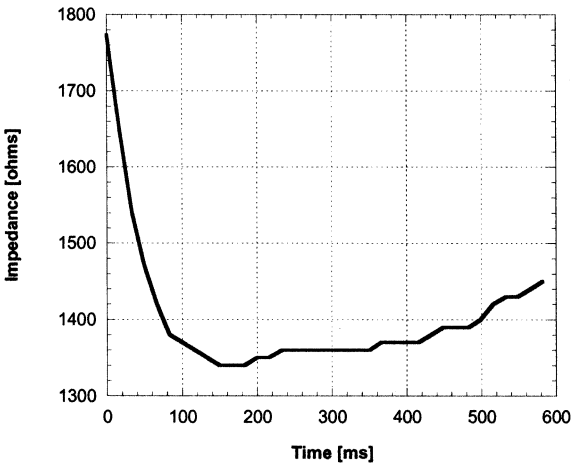

Fig. 10. Average impedance values obtained during the RF macropulse from *in vitro* porcine corneas. Power = 60%.

C. In Vivo Measurements

Preliminary impedance measurements at 60% power ($n = 5$) were obtained *in vivo* (Fig. 12). The initial impedance was

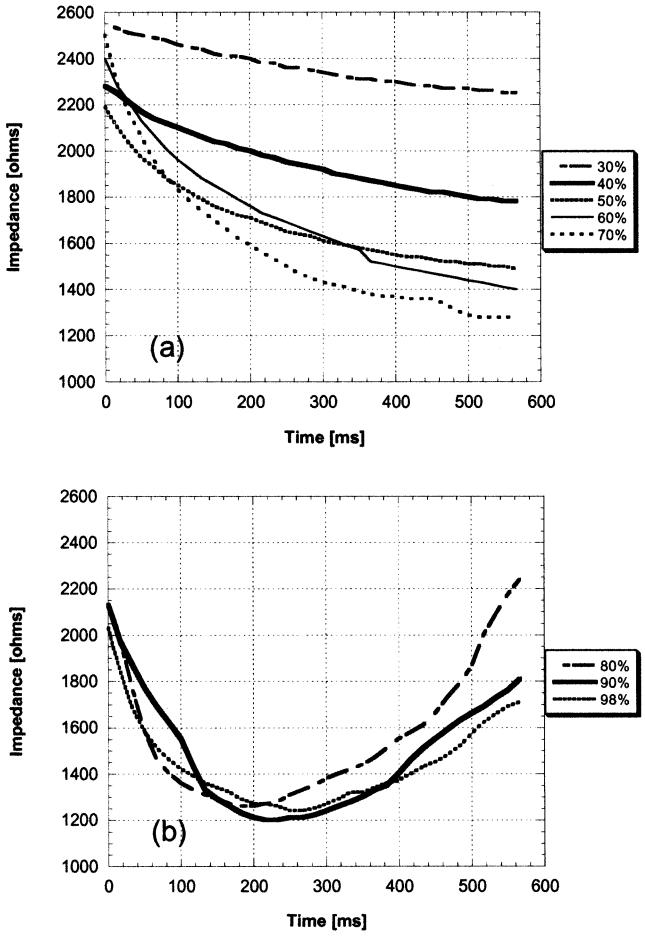

Fig. 11. Mean impedance data acquired during the RF macropulse at different power settings. (a) Power = 30%–70%. (b) Power = 80%–98%.

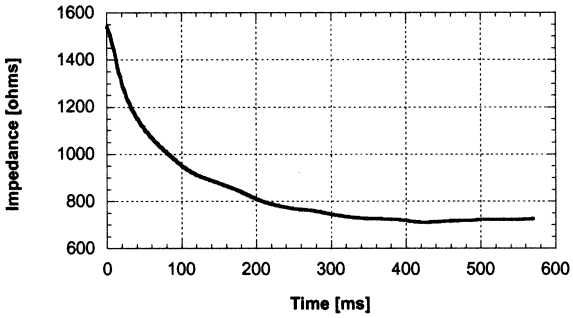

Fig. 12. Average impedance values obtained during the RF macropulse from *in vivo* porcine corneas. Power = 60%.

$\sim$1600 Ω, and during heating impedance values decreased to approximately 725 Ω.

IV. Discussion

Time-resolved measurements of dynamic changes in corneal impedance were obtained during RF heating of *in vitro* and *in vivo* porcine corneas. Initially, the dynamic behavior of impedance is dominated by heating along the electrode cylindrical shaft due to a thermally induced increase in electrical conductivity. At higher power settings, the impedance increases

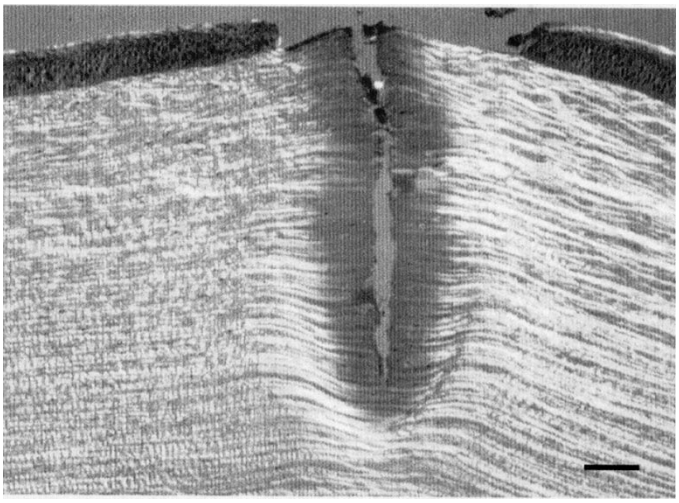

Fig. 13. Transmission polarization microscopy image of a histological section of porcine cornea after application of a RF lesion with the CK unit. Heat application was done *in vivo* with the clinical CK unit parameters (Power = 60%, macropulse duration = 600 ms). The hole created by the CK probe tip is readily apparent. The loss of birefringence (e.g., darker tissue) in the immediate region adjacent to the hole is indicative of the zone of thermal damage created by the RF macropulse. The solid black scale bar in the lower right corner represents 100 μm in length.

near the end of the 600-ms macropulse due to tissue desiccation. Knowledge of energy distribution dynamics is critical for accurate theoretical modeling of RF tissue heating. Histology obtained in a separate study [B. Choi, J. Kim, S. L. Thomsen, J. A. Pearce, and A. J. Welch, unpublished data] indicates that a zone of thermal damage extends laterally for approximately 125 μm (Fig. 13) This region is associated with thermal damage processes occurring at temperatures between 60 °C and 80 °C [8]. In regions of elevated temperature, the electrical conductivity was expected to increase with temperature, approximately 1%–2% per °C as determined for electrolytic solutions [9].

Increase in the mobility of charge carrier ion species (chiefly Na^+ and Cl^- ions) is the underlying physical cause. This can be explained from an analysis of carrier transport phenomena. The drift velocity U_d of a charge carrier is a direct function of mobility μ [m^2/V-s] and electric field strength E [V/m]

$$U_d = \mu E. \tag{1}$$

Mobility is proportional to temperature; thus, as temperature increases, mobility, and hence U_d, increase as well. Since electrical conductivity increases as drift velocity increases, corneal impedance will decrease as corneal temperature increases. Thus, for moderate temperature rises one would expect the conductivity to follow:

$$\sigma(T) = \sigma_o \exp(0.02[T - T_0]) \tag{2}$$

where σ_0 is the electrical conductivity at temperature T_0(°C). The decrease in impedance during the early heating phase (Figs. 10–12) is attributable to this effect.

Similar trends have been reported in the literature. Dadd *et al.* [10] measured impedance values of muscle, fat, liver, and brain at different tissue temperatures and during application of a low-power 500-kHz current. They found that impedance decreased as tissue temperature increased. However, no explanation was

provided for the impedance changes. At water bath temperatures of 80 °C, the impedance was noted to increase after the initial decrease. Impedance values of *in vitro* cow eyes were measured at different times during heating with the same RF system used in this study (RF frequency = 350 kHz) [Roger Stern, Stellartech Research Corporation, unpublished data]. At times of 27.5, 65, and 285 ms after onset of the macropulse, impedances of 1517, 1308, and 2422 Ω were measured. The increase in impedance at 285 ms was attributed to tissue coagulation.

In two sets of experiments, initial impedance values measured *in vitro* were 1775 Ω and ∼2200 Ω, which are in general agreement with each other. No corneal impedance values could be found in the literature to compare with those measured in this study. Jurgens *et al.* [11] measured the resistivity of *in vitro* porcine cornea samples to be between 0.39 and 0.48 Ω•m (conductivity between 2.1 and 2.56 S/m) over a 10 kHz to 10 MHz frequency range, a conductivity much higher than that of the 0.8% saline solution used in this study for electrode spectral measurements (1.39 S/m). For comparison, Pearce and Thomsen [12] reported electrical conductivities for *dura mater* (nearly pure collagen type I) of 0.26 ± 0.05 S/m in the transverse direction and 0.42 ± 0.17 S/m in the longitudinal direction.

To elevate the IOP of the *in vitro* eyes, saline was injected into the aqueous humor compartment of the eyes. Jurgens *et al.* [11] measured resistivities of balanced saline solution (0.625 Ω•m, or 1.6 S/m conductivity) and aqueous humor (0.60–0.67 Ω•m, or 1.5–1.6 S/m conductivity). The saline conductivities measured in the Jurgens *et al.* study and our study are similar. Also, the saline and aqueous humor conductivities are identical. Thus, we did not expect the presence of saline in the aqueous humor compartment to be a source of error in the impedance measurements.

Changes in delivered power led to differences in the shape of the impedance–time curve (Fig. 11). At 30% power, impedance stayed relatively constant during the macropulse. As power increased from 30% to 70%, impedance decreased at faster rates during RF application. Further increases in power led to an initial decrease in impedance followed by an increase that occurred approximately 200 ms after onset of the pulse.

Measurements by Torres *et al.* [13] suggested that an increase of tissue temperature above 60 °C may lead to significant water vaporization. This phenomenon was attributed to the exponential increase in water vapor pressure with temperature. For example, at 70 °C the vapor pressure is approximately ten times higher than it is at 25 °C. At higher temperatures, substantial tissue water is vaporized adjacent to the RF probe, removing the medium for translational motion of charge carriers, thus decreasing the carrier mobility. At higher temperatures (in the later stages of tissue heating) the expected increase in impedance is easily seen (Figs. 10 and 11). Power settings higher than 70% were sufficient to cause significant water vaporization and/or local coagulation to increase impedance [Fig. 11(a)].

Measurements at 60% power were acquired in two sets of experiments. In the initial experiments, corneal impedance decreased and then increased during the RF macropulse (Fig. 10). In the second set of experiments, corneal impedance at 60% power decreased but did not increase during the pulse [Fig. 11(a)]. This discrepancy may be due to differences in the following variables: 1) time *post-mortem*; 2) age of the pig at the time of sacrifice; and 3) storage and handling of the eyes at the distributor. These factors can lead to nonuniformities in corneal structure and integrity among the population of *in vitro* eyes used in this study.

Initial impedance values calculated for the *in vivo* eyes were lower than the values for *in vitro* eyes (∼1600 and ∼2000 Ω, respectively). More *in vivo* data is needed to arrive at a well-founded conclusion. Due to the lack of corneal impedance data in the literature, it is difficult to provide an adequate explanation for the discrepancy in impedance measured *in vitro* and *in vivo*. Since *in vitro* conditions differed from those *in vivo* in several ways (hydration, temperature, perfusion, IOP, etc.), the values measured *in vivo* should better represent the actual corneal impedance during the RF macropulse and stress the need to establish a relation between *in vitro* and *in vivo* data. Additional *in vivo* studies need to be conducted.

In light of the results of this study, our current hypothesis on how CK works is as follows: upon initiation of RF heating, there is a high current density at the sharp probe tip. This leads to rapid local desiccation of the cornea around the tip which results in an increase in impedance at the tip. This drives the current to the sides of the probe (e.g., pathway of least resistance). Since the probe shaft surface area is considerably greater than that of the probe tip, the current is spread over a larger area, resulting in a relatively small increase in heating. The slower temperature rise leads to an increase in conductivity [see (2)] along the probe tip. Thus, the combination of the decrease in impedance along the probe shaft with the increase in impedance at the probe tip results in an overall decrease in the measured impedance due to the larger surface area of the probe shaft. Eventually, as tissue coagulation and water loss along the shaft occurs, the measured impedance is expected to increase. Numerical modeling is currently underway to investigate the heat transfer and damage kinetics associated with CK heating.

V. Conclusion

Transient impedance curves were calculated during a RF macropulse emitted by a commercial unit under investigation for treatment of hyperopia. The initial impedance of the active electrode inserted into *in vitro* porcine corneas was approximately 2000 Ω. During the RF pulse, the impedance decreased initially due to an increase in charge carrier mobility in water. For power settings of 70% (e.g., maximum $V_{p-p} = 233$ V) and below, the measured impedance remained at a lower value during the entire macropulse. At higher powers, the impedance increased at approximately 200 ms after onset of the macropulse; this was attributed to significant water vaporization and coagulation of surrounding tissue. More *in vivo* studies need to be conducted to obtain an improved statistical comparison between *in vitro* and *in vivo* impedance trends.

Acknowledgment

The authors would like to thank P. Goth and L. Hood of Refractec, Inc., for providing the CK unit and assistance in aspects of the experimental design. They would also like to thank

Dr. G. Rylander and Dr. N. Wright for their assistance in conducting the experiments, and M. Martine and J. Letchworth for providing help during the *in vivo* studies. Finally, they would like to thank Dr. S. Thomsen for providing the histology section shown in Fig. 13.

REFERENCES

[1] C. Scerra, "Many techniques are available to tackle hyperopia: Most patients are pleased with refractive surgery despite not achieving 20/20 visual acuity," *Ophthalmol. Times*, May 1, 2000.

[2] T. Seiler, M. Matallana, and T. Bende, "Laser thermokeratoplasty by means of a pulsed holmium : YAG laser for hyperopic correction," *Refract. Corneal Surg.*, vol. 6, pp. 335–339, 1990.

[3] T. Seiler, "Ho : YAG laser thermokeratoplasty for hyperopia," *Ophthalmol. Clin. N. Amer.*, vol. 5, pp. 773–779, 1992.

[4] M. McDonald, P. Hersh, E. Manche, R. K. Maloney, J. Davidorf, and M. Sabry, "Conductive keratoplasty for the correction of low to moderate hyperopia: U.S. clinical trial 1-year results on 355 eyes," Ophthalmology, vol. 109, pp. 1978–1989, 2002, to be published.

[5] V. M. Thompson, T. Seiler, D. S. Durrie, and T. M. Cavanaugh, "Holmium : YAG laser thermokeratoplasty for hyperopia and astigmatism: An overview," *Refract. Corneal Surg.*, vol. 9s, pp. S134–S137, 1993.

[6] A. Chandonnet, R. Bazin, C. Sirois, and P. A. Belanger, "CO_2 laser annular thermokeratoplasty: A preliminary study," *Lasers Surg. Med.*, vol. 12, pp. 264–273, 1992.

[7] G. M. Hale and M. R. Querry, "Optical constants of water in the 200-nm to 200-mm region," *Appl. Opt.*, vol. 12, pp. 555–563, 1973.

[8] J. A. Pearce and S. L. Thomsen, "Rate process analysis of thermal damage," in *Optical–Thermal Response of Laser-Irradiated Tissue*, A. J. Welch and M. J. C. van Gemert, Eds. New York: Plenum, 1995.

[9] H. P. Schwann, "Biophysics of diathermy," in *Therapeutic Heat and Cold*, S. Licht, Ed. Baltimore, MD: Waverly, 1965.

[10] J. S. Dadd, T. P. Ryan, and R. Platt, "Tissue impedance as a function of temperature and time," *Biomed. Sci. Instrum.*, vol. 32, pp. 205–214, 1996.

[11] I. Jurgens, J. Rosell, and P. J. Riu, "Electrical impedance tomography of the eye: *In vitro* measurements of the cornea and the lens," *Physiol. Meas.*, vol. 17, pp. A187–A195, 1996.

[12] J. A. Pearce and S. Thomsen, "The effect of vessel architecture on fusion by radio frequency current," *Proc. SPIE*, vol. 3249, pp. 217–228, 1998.

[13] J. H. Torres, M. Motamedi, J. A. Pearce, and A. J. Welch, "Experimental evaluation of mathematical models for predicting the thermal response of tissue to laser irradiation," *Appl. Opt.*, vol. 32, pp. 597–606, 1993.

Bernard Choi was born in Chicago, IL, on September 3, 1974. He received the B.S. degree from Northwestern University, Evanston, IL, in 1996 and the M.S. and Ph.D. degrees from The University of Texas at Austin in 1998 and 2001, all in biomedical engineering.

He is currently a Beckman Fellow at Beckman Laser Institute, University of California, Irvine. His research interests include biomedical optics, optical imaging, biomedical heat transfer, diagnostic and therapeutic applications of lasers in dermatology, and numerical modeling of laser–tissue interactions.

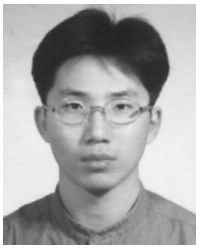

Jihoon Kim received the B.S. degree in electrical engineering from Konkuk University, Seoul, South Korea in 1999.

He is currently a graduate Research Assistant at The University of Texas at Austin. His research is focused on determining the coagulation pattern in cornea during conductive keratoplasty.

Ashley J. Welch received the B.E.E. degree from Texas Tech University in 1955, the M.Sc. degree in electrical engineering from Southern Methodist University (SMU), Dallas, TX, in 1959. He received the Ph.D. degree in electrical engineering from Rice University, Houston, TX, in 1964.

He is a Professor of Electrical and Computer Engineering and Biomedical Engineering and is the Marion E. Forsman Centennial Professor of Engineering at the University of Texas at Austin. He is an international authority on the optical and thermal response of tissue to laser irradiation. Basis analysis of laser–tissue interaction, OCT imaging, and feedback control have been employed to physically describe and enhance laser treatment of port wine stains, tissue welding, and skin resurfacing. Dr. Welch has published over 225 papers and book chapters describing his research. He, with Dr. van Gemert edited and contributed to the reference book *Optical–Thermal Response of Laser-Irradiated Tissue* (New York: Plenum, 1995).

Dr. Welch joined the University of Texas at Austin as an Assistant Professor in 1964. He has served as Director of the Hybrid Computer facility and Director of the Biomedical Engineering Program. Forty-two Ph.D. degree and 67 M.S. degree students have earned graduate degrees under him. He has been chairman or co-chairman for the Gordon Conference on Lasers in Surgery and Medicine, ASLMS annual meeting, Engineering Foundation's Future Directions for Lasers in Medicine and Surgery, SPIE annual meeting, and CLEO annual meeting. He has been an active reviewer for *Lasers in Surgery and Medicine* and serves on the Board of Directors for one term beginning in 1999. He has edited a special laser–tissue interaction issue of the IEEE TRANSACTIONS ON BIOMEDICAL ENGINEERING.

John A. Pearce (S'79–M'80–SM'92) received the B.S.M.E. degree and M.S.M.E. degrees from Clemson University, Clemson, SC, in 1964 and 1971, respectively, and the M.S.E.E. and Ph.D. degrees in electrical engineering from Purdue University, West Lafayette, IN, in 1977 and 1980, respectively.

He joined the faculty of electrical and computer engineering at the University of Texas at Austin in 1982, where he is presently the Temple Foundation Professor (#3) in electrical engineering. His research interests include applications of electromagnetic fields in tissues and in industrial processes, impedance measurements in tissues, and tissue thermal damage studies.